Journal of Engineering and Sustainable Development
http://jeasd.uomustansiriyah.edu.iq/index.php
https://doi.org/10.31272/jeasd.26.2.6

JEASD

Vol. 26, No. 02, March 2022
ISSN 2520-0917

# MAXIMUM POWER COEFFICIENT CONTROL OF A MICRO GRID-CONNECTED WIND ENERGY SYSTEM

***Mustafa M. Atiyah[1]** **Ali Jafer Mahdi[2]** **Kassim A. Al-Anbarri[1]**

1) Electrical Engineering Department, College of Engineering, Mustansiriyah University, Baghdad, Iraq
2) Department of Electrical and Electronic Engineering, University of Kerbala, Kerbala,, Iraq

***Received 26/8/2021*** ***Accepted in revised form 31/10/2021*** ***Published 1/3/2022***

**Abstract:** This paper proposed the integration of the wind energy system (WES) with the grid consists of a wind turbine, a permanent magnet synchronous generator (PMSG), a switch-mode rectifier (SMR) and a three-phase voltage source inverter (VSI). Optimal torque control (OTC) method is applied to the converter on the generator side for maximizing the power coefficient under the change in wind speeds. To synchronize the WES with the grid, another controller is applied to keep dc-bus voltage at constant value and to regulate active and reactive power transmitted into a grid. A system of WES connected into a grid is created and tested in the MATLAB/SIMULINK platform version 2019b. Comprehensive simulation results are used to analyze and verify the excellent performance of the suggested two- control strategy on the machine and grid side.

**Keywords**: *permanent magnet synchronous generator, switch-mode rectifier, wind energy system, grid Side convertor.*

## 1. Introduction

Few years ago, the energy demand has increased due to the rapid development of industrial sectors in various fields. This increase was associated with an increase in the rate of environmental pollation caused by traditional energy sources such as gas, coal, and other crude oil products. Therefore, the search for alternative energy sources has become an urgent necessity. Wind energy is considered one of the most growing and invested renewable energy sources in the world [1].

Many generators are used in wind energy applications, including the doubly-fed induction generator (DFIG), which is widely used, but the presence of the gearbox makes it suffer from many faults and requires constant maintenance and this may causes additional cost of the system and reduces reliability , PMSGs are an effective solution to the problems of the gearbox, as well as it has many advantages, including a built in permanent excitation, its ability to work at low wind speeds [2,3].

The power conversion utilized in WES applications can be divided into two topologies: (i) the first topology is back to back (BTB) converter, which consists of a three-phase rectifier controlled, connected to the generator side and a three-phase VSI connected to the grid side or load. The dc-link capacitor is connected

**Corresponding Author*: ahmem520@gmail.com

between them as it performs the isolation function between the generator side and the grid side [4, 5, 6].The second topology is SMR, which consists of uncontrolled three-phase rectifier connected with a DC-DC boost converter. The later configuration characterized by simplicity, low switching losses and unidirectional power flow as well as robust control to achieve maximum power point tracking (MPPT) [7,8].

The modeling and simulation study of variable speed PMSG had attracted many researchers. A simulation study of a variable speed PMSG based on wind turbine connected to the grid through two-leg switch BTB converter was presented it [9]. In Reference [10], a close loop control was also used to control the duty cycle of the boost converter for stand-alone system and connected to the network. Maximum power point tracking (MPPT) control for small scale PMSG wind turbine is designed by fuzzy logic control method (FLC) at different wind speed conditions in [11], power quality problems for variable speed wind turbines have been addressed in [12]. The electrical parameters identification of a PMSG such as (phase resistance, phase inductance and flux linkage) utilizing the PSO technique was implemented and investigated [13]. A comparison between three method for current regulator which is hysteresis-band current regulator (HBCR) and a PI current regulator (PICR) and improved PI-current regulator(IPICR) based on PSO was performed in small scale wind generation system (WGS) utilizing PMSG based on vertical axes-wind turbine (VAWT) to maximize output power in stand-alone system with resistive load [14]. A pitch angle and MPPT control strategy in WES using DFIG based on a wind turbine to handle with DC-link voltage overshooting and maintain faulty situations close to its nominal values under short-circuit was used in [15]. a MPPT control which is TSR based on perturbation and observation (P&O) with a variable step size in WES which comprise of PMSG connected to boost converter was suggested in [16].

This paper analyzed the performance of PMSGs based on wind turbine (WT) connected to a grid. SMR and three-phase VSI is used to connect PMSGs with the electrical grid. Two control strategies have been established via converter on the generator and grid side. The control signals for boost converter and VSI switches are generated by using pulse width modulation (PWM) and the dynamic performance of the system and effectiveness of two control strategies simulated by MATLAB/SIMULINK. The following are the significant contributions made by this work:

1. Applying MPPT algorithm on the SMR side to obtain maximum power from WES.
2. Stabilizing the DC-link voltage under the wind speed fluctuations, regulating active and reactive power transmitted to achieve unity power factor at different wind velocity.

## 2. System Modeling

### 2.1. Turbine Modeling

Wind Turbines (WT) are unable to catch all of the power produced by the wind, therefore wind-output turbine's power is given as [17]:

$$P_{wind-Turbine} = \frac{1}{2}\rho A C_p(\lambda,\beta)V_n^3 \quad (1)$$

Where: ρ air density ($K_{g/m^2}$), A swept area of a WT, $C_p$ is the turbine's power performance coefficient, which is governed by the rotor blade pitch angle $\beta$ (in degrees) and $V_n$ wind velocity (m/s).

The tip-speed- ratio λ is calculated as follows:

$$\lambda = \frac{\omega_m R}{V_n} \quad (2)$$

Where: $\omega_m$, $R$ rotor velocity (rad/s) and rotor radius (m) of a WT respectively.
A mechanical torque production by WT (Tm) can be represented as follows:

$$T_m = \frac{1}{2}\rho A C_p(\lambda,\beta)V_n^3\frac{1}{W_m} \quad (3)$$

Also the general equation is employed to represent the coefficient power $C_p$ $(\lambda, \beta)$ depending on the modeling WT characteristics stated in [18].

$$C_p(\lambda,\beta) = C_1(C_2/\lambda_i - C_3\beta - C_4)e^{-C_5/\lambda_i} + C_6\lambda \quad (4)$$

where; $C_1 - C_6$, are the empirical power coefficients parameters of the wind turbine

($C_1 = 0.5176$, $C_2 = 116$, $C_3 = 0.4$, $C_4 = 5$, $C_5 = 21$, $C_6 = 0.0068$).

$$\frac{1}{\lambda_i} = \frac{1}{\lambda + 0.008\beta} - \frac{0.035}{1+\beta^3} \quad (5)$$

The maximum value of $C_p$ is $C_{p-max}$ which is equal 0.48 in this work, this value is achieved when $\beta = 0$ $\lambda_{-opt} = 8.1$.
Therefore, in order to fully benefit from the variable speed-WES, the value of $\lambda$ must be maintained at the ideal value, which represents a unique value in each type of wind turbine and is calculated during the design of the wind turbine blades. When WT operates at the ideal tip speed ratio at all wind speeds, the operation point will be maximum value, which means obtaining the greatest power, achieving the MPPT, and $C_p$ will be at the maximum value despite the change in wind speeds, and this makes the power produced by the WT always the greatest possible Fig. 1.

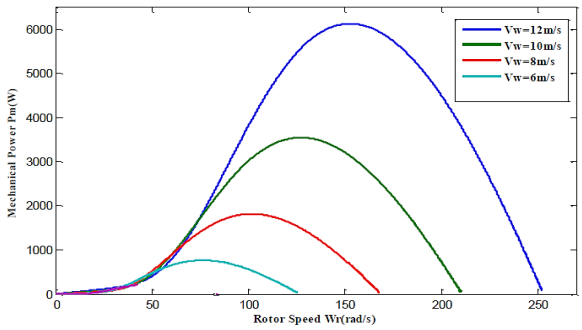


**Figure 1.** WT power versus rotor speed at different wind speeds

### 2.2. PMSG Model

The Equations that represent a PMSG's dynamic model in the d-q-0 reference frame can be expressed in equation (6) & (7) [19, 20]

$$V_{g-d} = (R_g + PL_d).I_d - W_e L_q I_q \quad (6)$$
$$V_{g-q} = (R_g + PL_q).I_q + W_e L_d I_d + W_e \emptyset_f \quad (7)$$

Where: $V_{g-d}, V_{g-q}$ are stator voltages along d-axis and q-axis, respectively. $I_d, I_q$ are stator current towards d-axis & q-axis, respectively. $R_g$ is the resistance of stator, $L_d, L_q$ is inductance on the dq-axis, $\emptyset_f$ is a flux-linkage developed by permanent magnet and $W_e$ electrical rotational speed for PMSG generator witch defined by :

$$\omega_e = P_a\omega_m \quad (8)$$

Where: $P_a$ is a number pole pairs for PMSG.
An electromagnetic torque can be represented by equation bellow:

$$T_{em} = \frac{3}{2}P_a[\emptyset_f I_q - (L_d - L_q)I_d I_q] \quad (9)$$

If the type of PMSG is surface mounted, therefore $(L_d = L_q)$ and electromagnetic torque can be represented as follow:

$$T_{em} = \frac{3}{2}P_a\emptyset_f I_q \quad (10)$$

## 3. Controlling System

### 3.1. MPPT Control

If a power coefficient ($C_p - max$=0.48) was maximum value and $\lambda$ at its optimum value ($\lambda$-opt), WES have the max amount of power .The max- power of a wind turbine could be written in the following form based on Equation (1).

$$P_{m-max}=0.5\ \rho\pi\ R^2 C_{p-max}(\lambda_{-opt}, \beta) v_n^3 \qquad (11)$$

In generator side or turbine side, the wind turbine's power coefficient can be adjusted. The power coefficient can be attained at max-value by adjusting a rotor speed at ideal point or through regulating the mechanical torque at maximum level. The characteristics of the mechanical torque versus rotor speed for wind turbine can be seen in Fig. 2 according for each variation in wind velocity, mechanical torque values vary due to change of the rotor speed of a WT and vary of wind speed.

$$T_{m-opt} = \frac{P_{m-max}}{W_m} = K_o w_m^2 \qquad (12)$$

Where: $K_o = \frac{0.5\ \rho\pi\ R^5 C_{p-max}}{\lambda\_opt\text{^}3}$

From dynamic equation of WT, reference electromagnetic torque $T_{em-ref}$ can be derived like in the following equation

$$T_{em-ref} = T_{m-opt} - \left(J\ \frac{dW_m}{dt} + B\ w_m\right) \qquad (13)$$

Where: J is overall inertia of WT, B is viscous friction factor. The electromagnetic torque could be regulated by adjusting a dc current passing through step up DC -DC converter. The dc-current reference for reference electromagnetic torque can be described as below:

$$I_{dc-ref}=\frac{T_{em-ref}\ W_m}{V_{dc}} \qquad (14)$$

Where: $V_{dc}$, is the output voltage of rectifier circuit. The duty cycle of a step up converter (D) is adjusted by a PI controller as shown in equation (15), also the block diagram of MPPT strategy can be seen in Fig. 3.

$$D = (K_p+\frac{K_i}{S})\ (\ I_{dc-ref}\text{-}I_{dc}) \qquad (15)$$

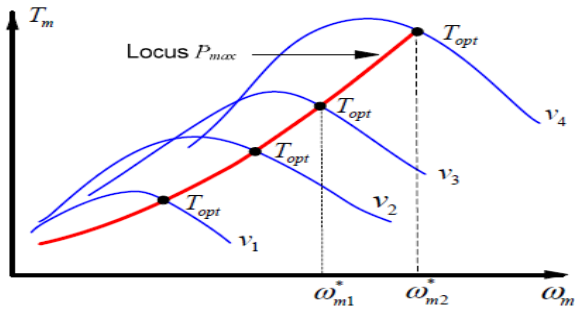


**Figure 2.** Characteristics of the mechanical torque vs rotor speed for different wind velocity.

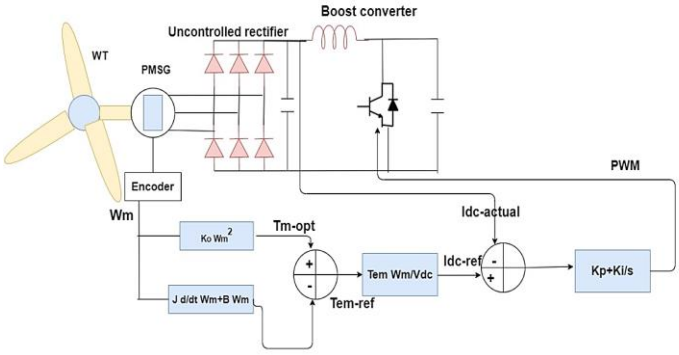


**Figure 3.** Scheme of MPPT algorithm

### 3.2. Control on the Inverter-Side

The objective of controlling in the grid-VSI side is to achieve two important goals for the process of incorporating the WES with the electrical network:

1. Due to the unstable nature of wind velocity, the voltage on the dc-link is constantly changing with the wind-speed conditions. Therefore, the control on the inverter-side should be regulates and maintains dc-link voltage according to the imposed design value.
2. Management and regulation of the reactive power and the active power supplied to the utility network, taking into account injection

of a power factor P.F are always equal to one [21].

The vector control (VC) method based on the PI controller is employed as approaches control used to regulate inverter-grid side. Fig.4 shows the overall schematic for the vector control that used in this work. As a result of VC, the reactive power infusion is controlled by a q axis loop, whereas the DC link voltage has been controlled by a d axis loop. Finally decoupling voltages are also provided to the current control loop outputs to accommodate for the cross-coupling effect caused by the output filter.

$$\begin{bmatrix} e_{a-inv} \\ e_{b-inv} \\ e_{c-inv} \end{bmatrix} = R_{-f} \begin{bmatrix} i_{ga} \\ i_{gb} \\ i_{gc} \end{bmatrix} + L_{-f} \frac{d}{dt} \begin{bmatrix} i_{ga} \\ i_{gb} \\ i_{gc} \end{bmatrix} + \begin{bmatrix} V_{a-grid} \\ V_{b-grid} \\ V_{c-grid} \end{bmatrix} \quad (16)$$

Where; $e_{a-inv}$ , $e_{b-inv}, e_{c-inv}$ inverter voltages , $V_{a-grid}$ , $V_{b-grid}, V_{c-grid}$ grid voltages, $i_{ga}$ , $i_{gb}, i_{gc}$ line currents and $R_{-f}, L_{-f}$ resistance and inductance of filter respectively.

By using synchronous reference dq-frame and space vector grid voltage is aligned on d-axis ($V_{grid-d} = V$ & $V_{grid-q} = 0$) and Eq. (16) can be written as:

$$e_{inv-d} = R_{-f} i_d + L_{-f} \frac{d}{dt} i_d - W L_{-f} i_q + V \quad (17)$$

$$e_{inv-q} = R_{-f} i_q + L_{-f} \frac{d}{dt} i_q + W L_{-f} i_d \quad (18)$$

where; $V_{grid-d}$ , $V_{grid-q}$ are grid voltages on the d-axis and q-axis respectively.

Also real power & reactive power can be described in dq rotating frame by the following equation:

$$P = \frac{3}{2} V i_d \quad (19)$$

$$Q = \frac{3}{2} V i_q \quad (20)$$

According to the block diagram of inverter-grid control in Fig.4 it can describe the equation of designing as follow:

$$error_{-Vdc}(t) = V_{dc-ref} - V_{dc-actual} \quad (21)$$

$$i_{d-ref} = K_p error_{-Vdc} + K_i \int error_{-Vdc} dt \quad (22)$$

$$error_{-id}(t) = i_{d-ref} - i_{d-actual} \quad (23)$$

$$error_{-iq}(t) = i_{q-ref} - i_{q-actual} \quad (24)$$

$$V_d^- = K_p \, error_{-id} + K_i \int error_{-id} \, dt \quad (25)$$

$$V_q^- = K_p \, error_{-iq} + K_i \int error_{-iq} \, dt \quad (26)$$

$$V_{d-ref} = V_d^- + V_{grid-d} \quad (27)$$

$$V_{q-ref} = V_q^- + V_{grid-q} \quad (28)$$

By using inverse Parks transformation we can obtain $V_a^*, V_b^*, V_c^*$ that used to provide the gate signals to trigger IGBTs switches of three-phase voltage source inverter.The control on the grid-inverter side can be seen in Fig. 4.

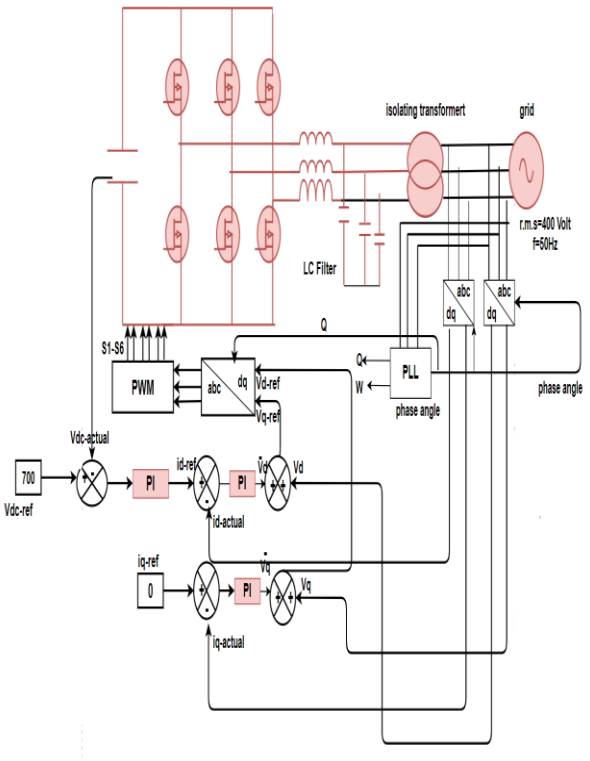


**Figure 4.** Schematic control on grid –VSI side

## 4. Simulation Results

MATLAB/SIMULINK is used to simulate the two proposed control strategies on the generator and grid side of a typical system. The special parameters that were used during the simulation are listed in Table (1), where the simulation was carried out through MATLAB/SIMULINK program. The total time of the simulation was 12 second.

**Table 1.** System Parameter

| PMSG parameters | | |
|---|---|---|
| $R_s$ = 0.425 Ω | $L_s$ = 0.00835 $H$ | $\lambda$ = 0.433 $wb$ |
| $J$ = 0.01197 | $\beta$ = 0.001189 | $P_{rated}$ = 6 kW |
| Parameter of wind turbine | | |
| *Rated wind speed =12 m/s* | R=2 m | $\beta$ = 0 |
| $\lambda_{optimal}$ = 8.1 | $\rho$ = 1.225 $kg/m^2$ | $Cp_{max}$ = 0.48 |
| Grid parameters | | |
| *R.M.S Line-Line Voltage* = 400 $V$ | $R$ = 0.1 Ω X/R ratio =7 | |
| DC link voltage = 700 $V$ | | |

The speed of the wind is changed as step size as seen in Fig.5.Wind speed is varied as bellow
From 0-3sec, the wind speed is about 12 m/s.
From 3-6sec, the wind speed is about 7m/s.
From 6-10sec, wind speed is about 12m/s too.
From 10-12sec, wind speed is about 9m/s.

The validity and reliability of the proposed control strategy called OTC to extract the maximum power from the WT and achieve MPPT can be checked under different operating conditions. This is done by observing the response of the wind turbine's $C_p$ and TSR. The maximum power of the WT is obtained at the optimum operating point when $C_p$ is at its maximum value and also TSR is at its optimum value. The value of $C_p$ and TSR for the proposed wind turbine model is 0.48 and 8.1 respectively. By using the OTC control strategy, the electromagnetic torque is controlled and $C_p$ of WT is always regulated at its maximum value despite changes in wind speed as shown in Fig.6 (a). Although the wind speed changes more than once during the simulation time, $C_p$ maintains its maximum value of about 0.48. What confirms the effectiveness of the OTC also is the response of the TSR as shown in Fig.6 (b) where it always maintains its optimum value of about 8.1 despite the wind speed variations. Fig.6(c) illustrates the output power from the PMSG at all wind speeds. When the WTs operates at the rated wind speed of 12m/s, the rated power is about 6000 watts, which corresponds to the generator data mentioned previously in Table (1), and this is evident during the simulation time from 0-3 seconds and from 6-10 seconds, where the wind speed is 12m/s. When the wind speed is 7m/s during the simulation time from 3-6 seconds, the power reaches about 1184 watts, and finally, the power reaches about 2524 watts at the simulation time from 10-12 seconds when the wind speed is 9m/s and this Another evidence of the accuracy and durability of the proposed control, as it confirms the achievement of the ideal operating point and reaching the MPP at all wind speeds entered.

Fig.6 (d) shows the reference speed that was created through the MPPT. We can see the reference speed at a value of 152.9 rad/sec when the wind speed is at its rated value of about 12m/s and this reference speed decreases when the wind speed decreases to become its value about 89 rad/sec when wind speed is 7m/s and reaches about 114rad/sec when wind speed is 9m/s. The MPPT is achieved when the speed is set at the above values by the proposed control method on the generator side. This indicates a good tracking of the reference speed values which the generator rotor must rotate at these values to achieve MPPT. Fig.6(e) shows the electromagnetic torque which changes with the change in wind speed, as it is set at its reference value that

achieves operation at maximum point of power when the wind speed is 12, the electromagnetic torque reaches about 40 N.m and then decreases when the wind speed decreases to reach 13.5 N.m at the wind speed 7m/s after that it increases to about 22 N.m when the wind speed 9m/s It is clear from the waveform of electromagnetic torque high response speed at each change in wind speed and this indicates the high tracking speed of the OTC proposed in this work. Fig.6 (f) depicts the duty cycle of a DC-DC converter. There is an ideal duty cycle value for each wind speed at which the turbine will operate at MPP. The duty cycle decreases as the wind speed increases.

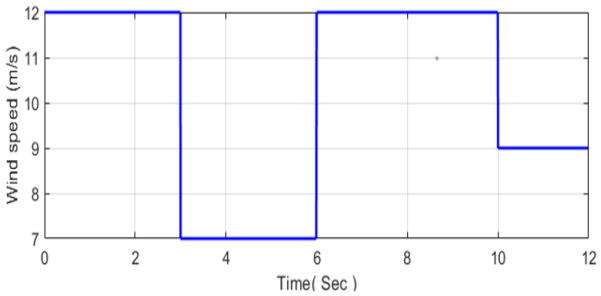


**Figure 5.** Variation of wind speed (m/s)

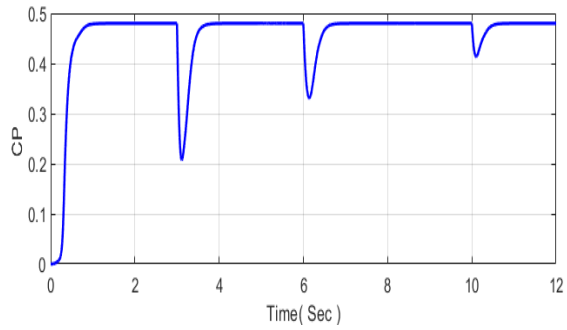


**(a)**

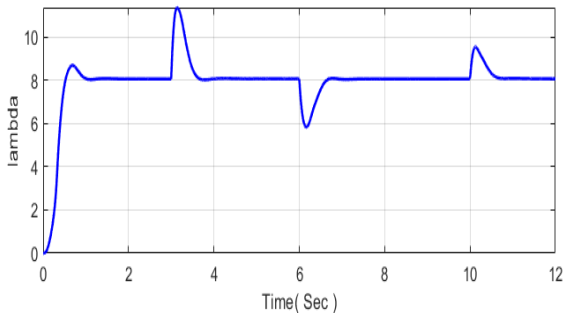


**(b)**

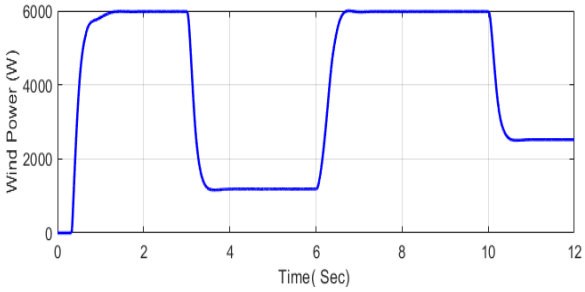


**(c)**

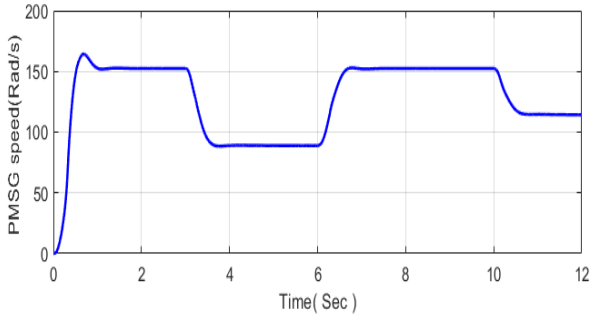


**(d)**

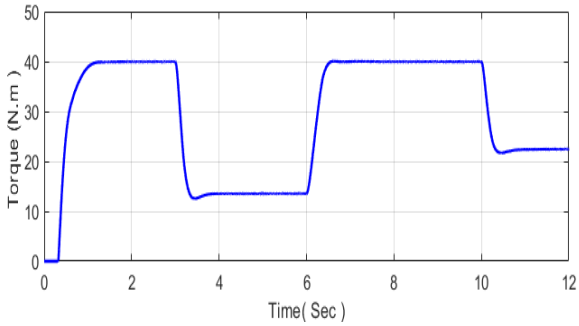


**(e)**

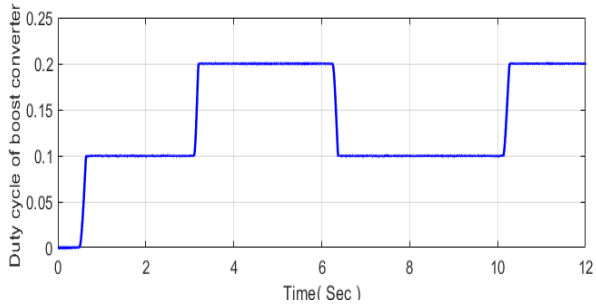


**(f)**

**Figure 6.** Simulation results of WES on the generator side, (a) Power coefficient, (b) Tip speed, (c) Output power (W), (d) Rotor speed (rad/s), (e) Electromagnetic torque (N/m), (f) Duty cycle of boost converter

The control method used from the grid side is the vector control based on PI controller, where the dc-link voltage is keeps at constant value which equal 700 volts in this paper, also the active power and reactive power are controlled and injected to the grid. Fig.7 (a) shows dc-link voltage waveform, which maintains its value constant at all wind speeds, as it appears stable and has few oscillations. Also, its response is fast when the wind speed changes. In addition, overshooting of waveform is within the permissible limits (less than 10%). Fig.7 (b) shows the waveform of the common coupling point (PCC) voltage, which is constant at all changes in wind speed, and this indicates the robustness of the control method used from the grid side. Fig.7(c) shows the PCC voltage under zooming. Fig.7 (d) shows the waveform of the PCC current injected to the grid that increases with increasing wind speed and decreases with decrease in wind speed. Fig.7 (e) shows the PCC current under zooming when wind speed is 12m/s. Fig.7 (f) illustrates the grid frequency which is maintained at 50 Hz in all operation conditions in spite of wind speed variation during simulation time .The THD of the grid current is about 3.31% (less than 5 %) according to the IEEE standard as shown in Fig. 7(g), this confirm good performance of the proposed control in the grid side. Finally Fig.8 shows the block diagram of MATLAB/SIMULINK of the proposed system in this study.

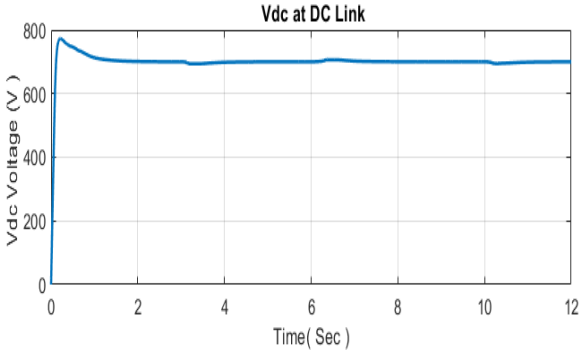


**(a)**

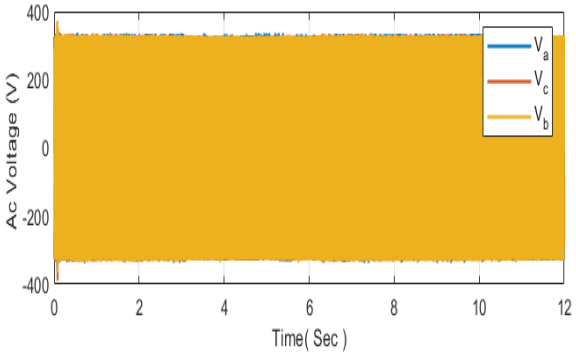


**(b)**

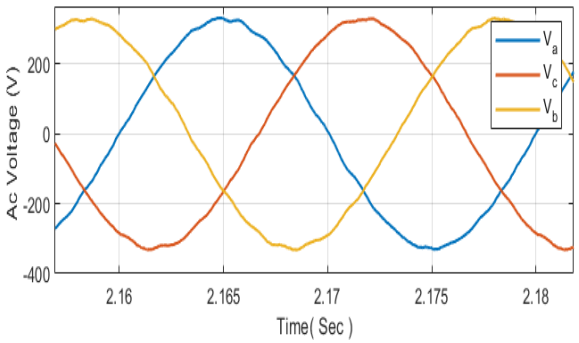


**(c)**

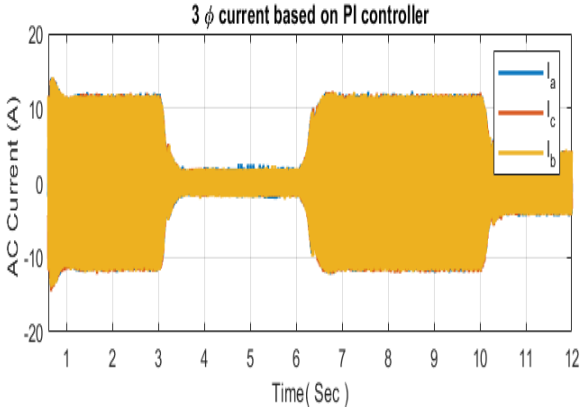


**(d)**

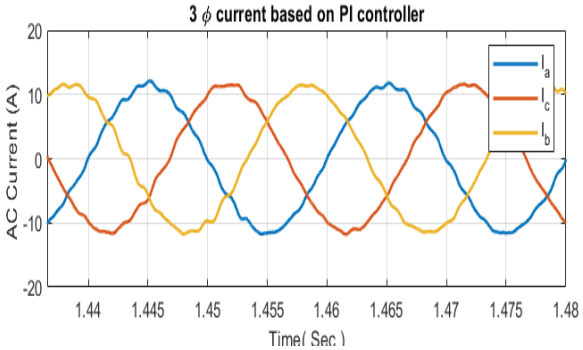


**(e)**

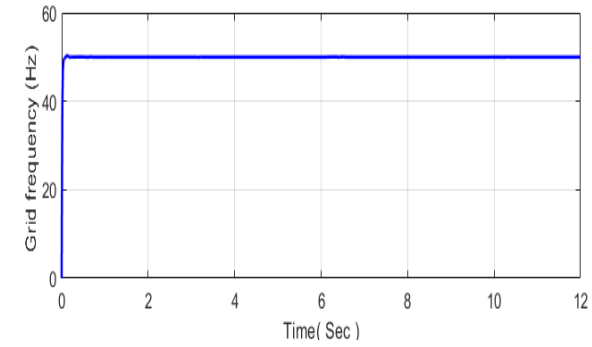


**(f)**

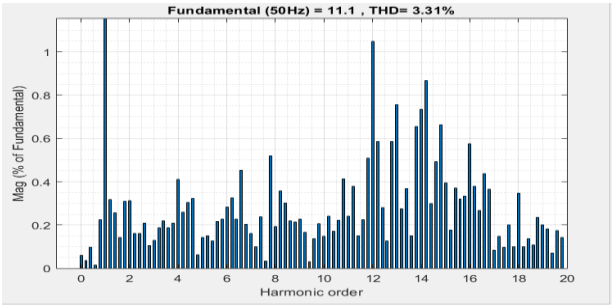


**(g)**

**Figure 7.** Simulation results of WES on the grid side, (a) dc link voltage (V), (b) PCC voltage (V), (c) PCC voltage under zoom (V), (d) PCC current (A), (e) PCC current under zoom (A), (f) Grid frequency, (g) Total harmonic distortion of grid current.

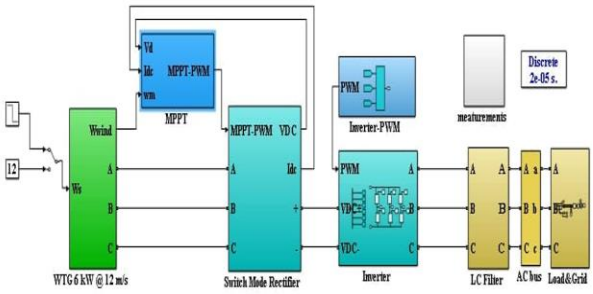


**Figure 8.** Simulink model of WES

## 5. Conclusion

A maximum power coefficient controller with a power synchronization controller is developed for a WES in this work. The entire system is tested in MATLAB/SIMULINK and it proved that the MPPT is implemented satisfactorily under real as well as ideal conditions. Simulation results have shown that the generator-side controller develops a clean DC voltage wave which consequently injects stable power to the PWM inverter. By using the grid side controller, the THD in the AC voltage wave is approximately 3.31% which is less than 5% for all wind speeds. Finally, power factor of the inverter is also close to unity.

## Conflict of interest

The authors confirm that there is no conflict of interest in the publishing of this article.

## 6. References

1. Kaldellis, J. K., & Apostolou, D. (2017). Life cycle energy and carbon footprint of offshore wind energy. Comparison with onshore counterpart. *Renewable Energy*, *108*, 72-84.
2. Zhang, Z., Hackl, C., Wang, F., Chen, Z., & Kennel, R. (2013, September). Encoderless model predictive control of back-to-back converter direct-drive permanent-magnet synchronous generator wind turbine systems. In *2013 15th European conference on power electronics and applications (EPE)* (pp. 1-10). IEEE.
3. Alepuz, S., Calle, A., Busquets-Monge, S., Kouro, S., & Wu, B. (2012). Use of stored energy in PMSG rotor inertia for low-voltage ride-through in back-to-back NPC converter-based wind power systems. *IEEE Transactions on Industrial Electronics*, *60*(5), 1787-1796.
4. Gajewski, P., & Pieńkowski, K. (2015). Control of a variable speed wind turbine system with PMSG generator. Maszyny Elektryczne: zeszyty problemowe.
5. Gajewski, P., & Pieńkowski, K. (2015). Analysis of a wind energy converter system with PMSG generator. Technical Transactions, Electronical Engineering Issue 1-E (8) 2015, 219–228.

6. Khater, F., & Omar, A. (2013). A review of direct driven PMSG for wind energy systems. *Journal of Energy and Power Engineering*, *7*(8).
7. Soumia, E. L., GUEDIRA, S., & EL ALAMI, N. (2014). Maximum power tracking control wind turbine based on permanent magnet synchronous generator with complete converter. *International Journal of Smart Grid and Clean Energy*, *3*(1), 15-21.
8. Hussein, M. M., Senjyu, T., Orabi, M., Wahab, M. A., & Hamada, M. M. (2012, December). Control of a variable speed stand alone wind energy supply system. In *2012 IEEE International Conference on Power and Energy (PECon)* (pp. 71-76). IEEE
9. Ahmed, A. A., Abdel-Latif, K. M., Eissa, M. M., Wasfy, S. M., & Malik, O. P. (2013, May). Study of characteristics of wind turbine PMSG with reduced switches count converters. In *2013 26th IEEE Canadian Conference on Electrical and Computer Engineering (CCECE)* (pp. 1-5). IEEE.
10. Vijayalakshmi, G., & Arutchelvi, M. (2014, March). Design and development of controller for PMSG based wind energy conversion system. In *2014 International Conference on Circuits, Power and Computing Technologies [ICCPCT-2014]* (pp. 573-578). IEEE.
11. Ngo, Q. V., Chai, Y., & Nguyen, T. T. (2020). The maximum power point tracking based-control system for small-scale wind turbine using fuzzy logic. International Journal of Electrical and Computer Engineering, 10(4), 3927.
12. Orlando, N. A., Liserre, M., Mastromauro, R. A., & Dell'Aquila, A. (2013). A survey of control issues in PMSG-based small wind-turbine systems. *IEEE transactions on Industrial Informatics*, *9*(3), 1211-1221.
13. Mahdi, A. J., Tang, W. H., & Wu, Q. H. (2010, December). Parameter identification of a PMSG using a PSO algorithm based on experimental tests. In 2010 1st International Conference on Energy, Power and Control (EPC-IQ) (pp. 39-44). IEEE.
14. Mahdi, A. J., Tang, W. H., Jiang, L., & Wu, Q. H. (2010, March). A Comparative study on variable-speed operations of a wind generation system using vector control. In International Conference on Renewable Energies and Power Quality, the 10th International Conference on Renewable Energies and Power Quality, University of Granada. Granada, Spain.
15. Nazir, M. S., Wang, Y., Mahdi, A. J., Sun, X., Zhang, C., & Abdalla, A. N. (2020). Improving the performance of doubly fed induction generator using fault tolerant control—a hierarchical approach. Applied Sciences, 10(3), 924.
16. Mahdi, A. J., Tang, W. H., & Wu, Q. H. (2011, September). Estimation of tip speed ratio using an adaptive perturbation and observation method for wind turbine generator systems. In IET Conference on Renewable Power Generation (RPG 2011) (pp. 1-6). IET.
17. Zhang, S., Tseng, K. J., Vilathgamuwa, D. M., Nguyen, T. D., & Wang, X. Y. (2010). Design of a robust grid interface system for PMSG-based wind turbine generators. *IEEE transactions on industrial electronics*, *58*(1), 316-328.
18. Abdullah, M. A., Yatim, A. H. M., & Tan, C. W. (2011, June). A study of maximum power point tracking algorithms for wind energy system. In *2011 IEEE Conference on Clean Energy and Technology (CET)* (pp. 321-326). IEEE.
19. Sagiraju, D. K. V., Obulesu, Y. P., & Choppavarapu, S. B. (2017). Dynamic performance improvement of standalone

battery integrated PMSG wind energy system using proportional resonant controller. Engineering science and technology, an international journal, 20(4), 1353-1365..

20. Shariatpanah, H., Fadaeinedjad, R., & Rashidinejad, M. (2013). A new model for PMSG-based wind turbine with yaw control. *IEEE transactions on energy conversion*, *28*(4), 929-937.
21. Zouheyr, D., Lotfi, B., Thierry, L., & Abdelmadjid, B. (2021). Grid Side Inverter Control for a Grid Connected Synchronous Generator Based Wind Turbine Experimental Emulator. European Journal of Electrical Engineering, 23(1), 1-7.